



## Research Article

# Drought stress responses deconstructed: A comprehensive approach for Norway spruce seedlings using high-throughput phenotyping with integrated metabolomics and transcriptomics



Muhammad Ahmad <sup>a</sup>, Sebastian Seitner <sup>b</sup>, Jakub Jez <sup>b</sup>, Ana Espinosa-Ruiz <sup>c</sup>, Esther Carrera <sup>c</sup>, Maria Ángeles Martínez-Godoy <sup>c</sup>, Jorge Baños <sup>c</sup>, Andrea Ganthaler <sup>d</sup>, Stefan Mayr <sup>d</sup>, Clara Priemer <sup>e</sup>, Emily Grubb <sup>a,f,1</sup>, Roman Ufimov <sup>a</sup>, Marcela van Loo <sup>a</sup>, Carlos Trujillo-Moya <sup>a,\*</sup>

<sup>a</sup> Austrian Research Centre for Forests BFW - Department of Forest Growth, Silviculture & Forest Genetics, Seckendorff-Gudent-Weg 8, 1131, Vienna, Austria

<sup>b</sup> Plant Sciences Facility, Vienna BioCenter Core Facilities GmbH (VBCF), Vienna, Austria

<sup>c</sup> Institute for Plant Molecular and Cell Biology (IBMCP), Consejo Superior de Investigaciones Científicas (CSIC) - Universidad Politécnica de Valencia (UPV), Calle Ingeniero Fausto Elio, S/n, 46022, Valencia, Spain

<sup>d</sup> University of Innsbruck, Department of Botany, Sternwartestraße 15, 6020, Innsbruck, Austria

<sup>e</sup> Div. Molecular Systems Biology, Dep. of Functional and Evolutionary Ecology, University of Vienna, Djerassiplatz 1, 1030, Vienna, Austria

<sup>f</sup> Institute for Hygiene and Applied Immunology, Center for Pathophysiology, Infection and Immunology, Medical University of Vienna, Vienna, Austria

## ARTICLE INFO

## Keywords:

Norway spruce seedlings  
Picea abies  
Drought stress  
High-throughput phenotyping  
Climate change

## ABSTRACT

Norway spruce (*Picea abies* Karst L.) is one of the most ecologically and economically significant tree species in Europe, accounting for nearly half of the continent's forest economic value. However, drought is a significant stress factor associated with increasing Norway spruce mortality across Europe. Provenance trials, a traditional approach to assess adaptive variation, face limitations stemming from the finite number of sites, seed sources involved, and their required labor-intensive nature. In response, we developed a comprehensive multisensor high-throughput phenotyping method and integrated it with metabolomics, transcriptomics, and anatomical analyses to study the drought stress responses in two climatically contrasting but geographically proximal provenances at the seedling stage by exposing them to drought stress for a period of 21 days. Based on more than 50 physiological and growth-related traits assessed by the phenotyping platform, it was possible to characterize early and late drought stress responses. Consistent with phenotypic data, mRNA-seq, and metabolic profiles revealed apparent differences between treatments. While during the drought stress the metabolic data indicated an increased production of ABA,  $\alpha$ -tocopherol, zeaxanthin, lutein, and phenolics, mRNA-seq showed modulation of related pathways and downregulation of photosystem transcripts. Although drought responses were largely conserved between the two provenances, they differed phenotypically in traits related to the activation of re-oxidation of the plastoquinone pool, and molecularly in transcriptional and phenolic profiles. In conclusion, our study demonstrates the potential of the high-throughput phenotyping approach for evaluating drought stress adaptation in Norway spruce thus accelerating the screening and selection of best adapted provenances.

**Abbreviations:**  $\Psi_s$ , Soil water potential;  $\Phi$ PSII\_Lss, Steady-state operating efficiency of photosystem II; ABA, Abscisic acid; Chl a, b, Chlorophyll a, b; CHLF, Chlorophyll fluorescence; CKs, Cytokinins; DEGs, Differentially expressed genes; DHZ, Dihydrozeatin; Fp, Peak fluorescence; Fo, Minimal fluorescence; Ft\_Ln, Instantaneous fluorescence at saturating light pulse Ln; Fv/Fm, Maximum quantum yield of PSII; Ft\_Lss, Steady-state terminal fluorescence; GA, Gibberellic acid; GO, Gene ontology; HTPP, High-throughput plant phenotyping; IAA, Indole acetic acid; iP, Isopentenyladenine; JA, jasmonate; KEGG, Kyoto Encyclopedia of Genes and Genomes; MCARI, Modified chlorophyll absorption in reflectance index; NDVI, NDVI2, Normalized difference vegetation index; NPQ, Non-photochemical quenching; NPQ\_Lss, steady-state NPQ; PCA, Principal component analysis; OSAVI, Optimized soil adjusted vegetation index; PRI, Photochemical reflectance index; PSRI, Plant senescence reflectance index; RGB, Red, Green, Blue; R.H., Relative humidity; SA, Salicylic acid; SNPs, Single nucleotides polymorphisms; SIPI, Structure insensitive pigment index; SWIR, Short-wave infrared; tZ, *trans*-zeatin; VNIR, Visible near infrared; VOCs, Volatile organic compounds.

\* Corresponding author.

E-mail address: [carlos.trujillo-moya@bfw.gv.at](mailto:carlos.trujillo-moya@bfw.gv.at) (C. Trujillo-Moya).

<sup>1</sup> Current affiliation: Institute for Hygiene and Applied Immunology, Center for Pathophysiology, Infection and Immunology, Medical University of Vienna, Vienna, Austria.

<https://doi.org/10.1016/j.plaphe.2025.100037>

Received 6 August 2024; Received in revised form 20 February 2025; Accepted 22 March 2025

Available online 31 March 2025

2643-6515/© 2025 The Authors. Published by Elsevier B.V. on behalf of Nanjing Agricultural University. This is an open access article under the CC BY-NC-ND license (<http://creativecommons.org/licenses/by-nc-nd/4.0/>).

## 1. Introduction

Drought is a major stress factor associated with rapidly increasing tree mortality across Europe [1,2]. With the projected climate change, drought is expected to increase in frequency, intensity, and duration [3,4], further predisposing trees to secondary damage caused by pests and pathogens. The speed of climate change is forecasted to outpace the ability of forest species to adapt in time [5]. Norway spruce (*Picea abies* Karst L.), which is ecologically and economically one of the most important forest species in Europe, is highly vulnerable to drought [2,5,6]. Lower precipitation and reduced soil water availability during summer have been shown to severely reduce Norway spruce growth [2,7]. Therefore, identifying adaptive populations and elucidating the genetic architecture and mechanistic basis of drought tolerance in Norway spruce provenances is of utmost importance.

For Norway spruce, studying drought tolerance at the seedlings stage has mainly relied on height, and stem diameter measurements which are measured manually in a labor-intensive manner [8–10]. This allows only a limited number of phenotypic traits to be assessed for relatively few individuals [11–13]. Additionally, in such studies, drought stress cannot be homogeneously applied or scaled up for many provenances. To meet current and future demands, the forestry sector needs to adapt rapid, reliable, and non-invasive methods that have the potential to screen large numbers of provenances in a timely and cost-efficient manner. These methods need further integration with large-scale genomic and transcriptomic projects to dissect the genetic and mechanistic basis of drought tolerance and to fasten the tree breeding programs.

Multisensor automated high-throughput plant phenotyping (HTPP) can play a critical role in this regard. It allows non-invasive monitoring of a wide range of phenotypes in thousands of individuals over time [10]. For instance, RGB imaging provides insights into plant growth rate, size, and morphology [10,14]. A 3D laser scanner enables assessment of plant height and other structural traits [15]. In contrast, chlorophyll fluorescence (CHLF) imaging offers insight into photosystem II (PSII) performance. Beyond growth and physiological traits, hyperspectral sensors (VNIR, SWIR) enhance phenotypic coverage by estimating pigment composition and tissue water content [16–18]. As drought affects all these plant functions, its complex nature cannot be fully captured by a single sensor, necessitating a multisensor approach for comprehensive drought assessment [19].

While these sensors capture real-time phenotypes, integrating HTPP with metabolomics and transcriptomics reveal biochemical and genetic mechanisms underlying drought adaptation [20]. Among others, metabolomics identifies hormones regulating plant growth and signaling, as well as stress-related metabolites involved in photoprotection and oxidative stress mitigation. Meanwhile, transcriptomics uncovers key structural and regulatory genes underlying these responses [20]. This multi-layered approach deepens our understanding of drought responses and provides a framework for selecting potentially drought-adaptive populations.

Application of HTPP in model plants (e.g., *Arabidopsis*) and crop species has already resulted in closing the gap between genotype and phenotype [21,22]. In contrast, in the forestry sector, HTPP is still in its early stages as only a handful of studies could be found in the literature [23–25]. While RGB and hyperspectral imaging have been used to assess drought stress responses in aforementioned studies, no study has used an integrative approach that simultaneously assesses plant growth, PSII efficiency, and vegetation indices in a high-throughput manner in any forest tree species. Furthermore, even in crop species, there are only a few studies that have complemented multisensor phenomics data with metabolomics and transcriptomics [20,26]. Integration of phenomics data with other omics approaches is required to comprehensively characterize drought-related phenotypes along with molecular and metabolic pathways that regulate these responses [15].

In the present study, we established for the first time an HTPP method to study drought stress responses in Norway spruce at the seedling stage.

The seedlings stage is the most critical developmental phase exposed to high selection pressure owing to limited root space, restricted water reservoirs, and competition with other plants. This makes seedlings especially high risk for drought stress. We exposed eight-week-old seedlings from two climatically contrasting provenances to severe drought stress. Using multiple sensors (CHLF, RGB, VNIR, SWIR, and 3D scanner), we monitored their responses at up to 10 time points. We further complemented the phenotypic measurements with shoot metabolomics (pigments, tocopherols, phenolics, terpenoids, and phytohormones), mRNA-seq profiles and stem anatomical analyses. Our specific aims were to establish a standardized HTPP method to study drought stress responses in Norway spruce seedlings and to integrate it with other omics data sets to better understand the mechanistic basis of observed phenotypic responses. Our results indicate that HTPP when integrated with other omics approaches is a valuable tool to study drought stress responses in seedlings of Norway spruce.

## 2. Materials and methods

### 2.1. Experimental design

The experiment was set up in a completely randomized fashion and consisted of three factors. The first factor was provenance (i.e., seeds originated from a population of more than one tree), as we obtained two climatically contrasting provenances (P1 and P2) within the natural range of *P. abies* from Poland. Provenance P1 (higher altitude) and P2 (lower altitude) are characterized by a climate as relatively wet and cold for the origin of the P1 site, and relatively warm and dry for the P2 site (Figs. S1a and b). The second factor was the treatment consisting of two levels: well-watered (soil water potential =  $\Psi_s = -0.02$  MPa) and drought ( $\Psi_s = -2.14$  MPa) (Fig. S1c). Drought was applied by maintaining  $\Psi_s$  at  $-2.14$  MPa for 21 days. We note that seedlings of P1 and P2 started to experience drought prior to reaching the target  $\Psi_s$ . Nevertheless, for consistency, we always refer to day 0 when target  $\Psi_s$  was reached in 35 % of plants (100 % plants on day 1), and 21 days of drought were counted based on this reference. The third factor was time, where HTPP was performed for a period of 10 and nine days ( $-2, 0, 3, 5, 7, 10, 12, 14, 17,$  and  $21$  days) for CHLF/RGB and VNIR/SWIR, respectively. In addition, 3D scanning of whole seedlings was performed at 10, 12, 14, 17, and 21 days after target  $\Psi_s$  was reached. A layout of the experimental design is depicted in Fig. S1d. For HTPP, we randomly selected 20 individuals from each treatment and provenance. The same 80 individuals (20 per treatment and origin) were then phenotyped at 9–10 different time points using a HTPP at PHENOPlant (Plant Science Facility, VBCF Vienna BioCenter Core Facilities GmbH). For sampling, pools of 19–24 individuals per provenance, treatment, and time point were harvested each week for a period of 21 days, resulting in four-time points (day 0, 7, 14, and 21). The last time point (day 21) included only those plants that were phenotyped for the entire duration of the drought stress period. Because the seedlings were small and had a limited amount of tissue available for molecular analyses, a pooling strategy was used. This involved combining 19–24 individuals from each time point, treatment, and provenance, resulting in a total of 16 pooled samples (4 time points \* 2 provenances \* 2 treatments). Aerial tissues at the stem-needles junction were cut directly with scissors and immediately flash-frozen in liquid nitrogen. Samples were then stored at  $-80$  °C until further processing. Samples were homogenized in liquid nitrogen using a pestle and mortar. Three technical replicates were taken from each pool and used for phytohormones, volatiles, phenolics, chlorophylls, total carotenoids, and mRNA-seq analysis.

### 2.2. Plant material and growth conditions

The experiment was conducted in the controlled climatic chamber of the Plant Science Facility (VBCF GmbH). Seeds of two provenances were obtained from the Kostrzyca Forest Gene Bank (<https://www.las>

y.gov.pl/). Seeds (5 seeds/pot) of both provenances were sown in pots (7 X 7 × 8 cm, Poppelman TEKU DE) filled with 80 g (oven dry weight  $37.6 \pm 1.14$  g) of a freshly sieved substrate (Gramoflor Topf + TonXL, Gramoflor GmbH & Co. KG, Germany). Prior to the experiment,  $\Psi_s$  was calculated based on the curve provided in Fig. S1c. Soil water retention parameters of the used substrates were derived by the extended evaporation method [27] using commercial HYPROP-devices ([www.metergroup.com](http://www.metergroup.com)). The measurement cores (n = 3) were packed with the same bulk density and water content as it was foreseen for the pots for the experiment. Prior to sowing, the soil was watered to ~70 % of the field capacity ( $\Psi_s = 22 \times 10^{-4}$  MPa) and was kept close to this level during the first six weeks of seedling growth. To control for insect infestation, a solution containing *Bacillus thuringiensis* was applied together with the first watering. Seeds were then allowed to germinate under long-day (16 h light/8 h dark) and low light conditions ( $100 \mu\text{mol m}^{-2} \text{s}^{-1}$  at the substrate level) at a constant temperature of 21 °C. Relative humidity (R.H.) was maintained at 100 % for the duration of germination (two weeks). To achieve 100 % R.H., trays containing pots were covered with transparent plastic domes. After germination (14 days after sowing), the domes were removed, and the seedlings were singularized by removing extra seedlings to one plant per pot. Following that, the R.H. was then adjusted to 60 %, and the light intensity was gradually increased to  $200 \mu\text{mol m}^{-2} \text{s}^{-1}$  at the substrate level. These conditions were then maintained for the duration of the experiment.

### 2.3. Drought simulation

Six weeks after sowing, the  $\Psi_s$  was gradually reduced to  $-0.02$  MPa. Out of 380 plants (190 per provenance) grown in the experiment, half of the seedlings (n = 95 per treatment and provenance) from each provenance were then randomly assigned to the drought or well-watered treatment. To simulate drought stress, the  $\Psi_s$  was further reduced to  $-2.14$  MPa and then was maintained at this level for 21 days by manually weighing all the pots daily and replenishing the evapotranspiration losses. Well-watered plants were maintained at  $-0.02$  MPa by manually weighing and compensating for daily evapotranspiration losses.

### 2.4. High-throughput phenotyping

Plants were imaged every two to three days for three weeks using a PSI PlantScreen Modular System (Photon System Instruments spol. s r.o., Drasov, Czech Republic) located at the Plant Science facility of the VBCF, PHENOPlant. Trays of 20 pots were manually loaded into the imaging system, each tray was imaged from the top using RGB, CHLF, 3D, and hyperspectral cameras as described below. All cameras were mounted on horizontally movable frames that adjust to the height of the plants.

### 2.5. RGB imaging

RGB images were acquired by PSI RGB camera using a 12.36-megapixel CMOS sensor (Sony IMX253LQR-C) and fitted with a Samyang 16 mm f2 AS UMC CS lens. The images have a size of 4112 x 3006 pixels and were output in.png format. The fisheye correction was performed automatically by the system. Illumination was from above using cool white LEDs.

### 2.6. Chlorophyll fluorescence imaging

For CHLF imaging, plants were dark adapted for 20 min and imaged using a quenching protocol displayed in Fig. S2. Briefly, after dark adaptation,  $F_0$  under the dark was measured by applying 5 s of a weak light beam ( $0.02 \mu\text{mol m}^{-2}$  in 10  $\mu\text{s}$  pulses). Subsequently,  $F_m$  under dark was measured by applying a saturating pulse of  $2544 \mu\text{mol m}^{-2} \text{s}^{-1}$  for 800 ms. Following this, plants were relaxed in the dark for ~3 s and then exposed to cool-white actinic light for 60 s. During actinic light exposure, three additional saturating pulses (L1, L2, and Lss) at 27.8, 47.8, and

67.8 s were applied to measure maximum ( $F_m$ , Ln) and instantaneous/steady-state fluorescence ( $F_t$ , Ln;  $F_t$ , Lss) in a light-adapted state. Images were acquired with a PSI FluorCam FC-800MF PAM camera containing a 1.4-megapixel CCD sensor with an image resolution of 1360 x 1024 pixels. The camera was fitted with a 695–770 nm chlorophyll fluorescence filter. Image frames were captured every 50000  $\mu\text{s}$  throughout the imaging protocol and output as 16-bit binary images. Images of measured and calculated parameters (Table S1) were generated automatically by the system as binary float images.

### 2.7. Hyperspectral imaging

Hyperspectral images were acquired by a VNIR and SWIR camera mounted adjacent to each other on a movable gantry. Illumination for both cameras was provided by a halogen lamp mounted adjacent to the cameras. VNIR images were acquired by a line-scanning hyperspectral camera covering 350 nm–900 nm with a spectral resolution of 0.8 nm. SWIR images were acquired by a second-line scanning hyperspectral camera covering 900 nm–1700 nm with a spectral resolution of 2 nm. Further detailed description of image analysis is described in [Supplementary materials and methods](#).

### 2.8. Statistical analysis for high-throughput phenotyping

As a first exploratory analysis, PCA was performed using 56-traits derived from CHLF (n = 41 traits), RGB (n = 7), SWIR (n = 1) and VNIR (n = 7) sensors. These traits and their definitions are provided in Table S2. For detailed analysis and description of traits, we focused on variables that have well-defined biological explanations [20,28,29]. PCA was performed using mean values of each trait per provenance, time, and treatment. For RGB and CHLF traits, a non-parametric Wilcoxon test was applied to compare the treatments of each provenance at the respective time points. The resulting p-values were corrected by Bonferroni correction. For hyperspectral data, a t-test was applied at each time point for each wavelength. Further details of statistical analysis and the number of replicates used for each analysis are presented in Figure legends. All analyses were performed in R studio (v2022.02.3 + 492; (RStudio, 2020)). The following R packages were used for the analysis and plotting: ggpubr (v 0.6), rstatix (v 0.7.2), and ggplot2 (v 3.4.4).

### 2.9. Phytohormonal, phenolics, and terpenoids analysis

Frozen powdered tissues in triplicates were used for each analysis. Further details on the methodological approach are described in [Supplementary materials and methods](#).

### 2.10. Carotenoids, chlorophylls and tocopherol quantification

Carotenoids, chlorophylls and tocopherols were analyzed as described in [Supplementary materials and methods](#). Due to limited amount of available material, only one replicate could be analyzed for each of the four time points (0, 7, 14, 21). For statistical analysis, we pooled samples from each time-point thus making 4 replicates. This method allowed us to maximize the available data while ensuring a meaningful comparison. Data was analyzed using two-way ANOVA followed by the Tukey HSD test for multiple comparisons.

### 2.11. RNA isolation, library preparation, sequencing and analysis

RNA isolation, library prep, sequencing, and data analysis were performed as described in [Supplementary materials and methods](#).

### 2.12. Anatomy

Stem anatomical analyses were carried out on 12 samples per provenance and treatment from the last time point. Segments approximately

2 cm long were cut from the stem just above the soil surface at the base and soaked in ethanol (70 %) for approximately two months prior to analysis. Thin cross sections (15  $\mu\text{m}$ ) were then cut using a microtome (Sledge Microtome G.S.L. 1, Schenkung Dapples, Zurich, Switzerland) and images of the entire section were gained with a digital microscope camera (Gryphax Arktur 8, Jenoptik, Jena, Germany) connected to a light microscope (Olympus BX 41, System Microscope, Olympus Austria, Vienna, Austria). Using the image analysis software ImageJ (ImageJ 1.45, public domain, National Institutes of Health (NIH), Bethesda, MD, USA), the following parameters were measured along a radial transect from pith to epidermis: total stem width, the width of central pith, xylem, phloem, bark (chlorenchyma, collenchyma, and periderm) and epidermis, number of resin channels, number of tracheid rows formed and mean radial tracheid diameter (calculated as the quotient of xylem width and the number of cell rows formed by the seedling).

### 3. Results

#### 3.1. HTPP-derived traits capture treatment, temporal, and genetic components of drought stress responses in Norway spruce seedlings

To assess the effectiveness of HTPP in studying drought responses of Norway spruce, we exposed two climatically contrasting provenances (P1 and P2) to 21 days of drought stress. During this period, plants were phenotyped using RGB, CHLF, VNIR, and SWIR sensors, generating 56 traits related to growth, photosynthesis, tissue water status, and vegetation indices (Fig. S3; Table S2).

A PCA based on mean trait values at each time point revealed clustering by treatment along the PC1 (56.7 % variance). This separation was primarily driven by traits related to the light-harvesting ability of PSII ( $\Phi\text{PSII}$ ), growth, and tissue water contents, as captured by CHLF, RGB, and SWIR sensors, respectively. Temporal drought progression was captured by PC2 (26.2 % variance) where early drought responses were associated with CHLF-derived non-photochemical quenching (NPQ), reflecting photoprotection. Meanwhile, later drought responses were associated with CHLF-derived minimal fluorescence ( $F_0$ ,  $F_0\text{-Ln}$ ), reflecting PSII damage. PC3 (5.7 % variance) distinguished the two provenances under drought with CHLF-derived peak fluorescence ( $F_p$ ), steady-state/instantaneous fluorescence ( $F_t\text{-L1}$ ,  $F_t\text{-L2}$ ,  $F_t\text{-Lss}$ ), and  $F_0$  were major contributors (Fig. 1, S4, Table S3). Relative values showed that  $F_0$  was more affected in P1 than in P2, while the other traits were more affected in P2 (Fig. S5), suggesting differences in plastoquinone redox balance.

PC loadings and correlation analysis revealed strong relationships among traits within individual sensors, suggesting redundancy. However, traits between sensors exhibited lower correlations (particularly CHLF and RGB), highlighting complementarity as each sensor captured distinct aspects of drought stress (Fig. S4). Taken together, these findings demonstrate the advantage of a multisensor approach, where complementary contributions from each sensor synergize to enable a more comprehensive assessment of drought-induced changes and provenance-specific differences.

#### 3.2. RGB imaging and 3D scanning reveals growth differences in Norway spruce provenances

To monitor the growth dynamics of Norway spruce seedlings, we measured the canopy area (green area in  $\text{mm}^2$  of the plant that can be seen from top view; Table S2) and height using an RGB top-view camera and a 3D scanner, respectively. Both provenances showed significant ( $P < 0.05$ ) growth reduction under drought stress, with neither maintaining growth comparable to well-watered seedlings (Fig. 2a and b). While absolute differences in height and canopy area between provenances were apparent under both treatments, the differences under drought were not significant. However, in relative terms, both canopy area and height significantly ( $P < 0.05$ ) differed between provenances

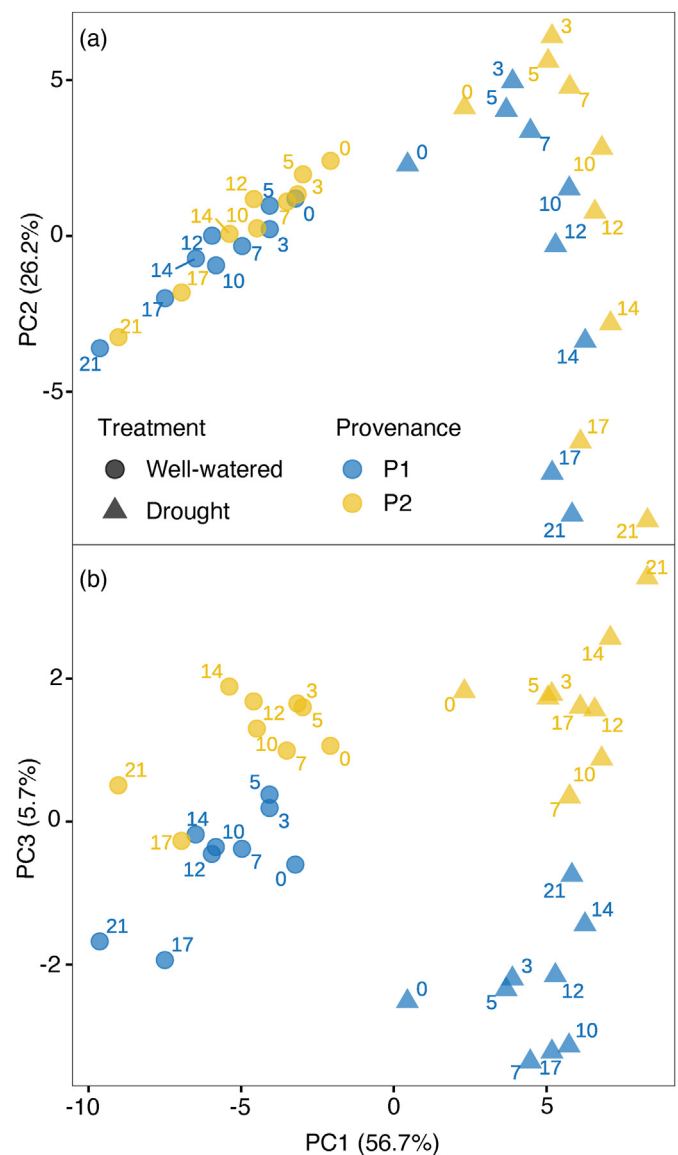


**Fig. 1.** Principal component analysis (PCA) of high-throughput plant phenotyping (HTPP) derived traits capturing differences between treatments, provenances, and time. (a) PC1 vs PC2 (b) PC1 vs PC3. Each dot or triangle is an individual time point as indicated by numbering. PCA was derived using average values ( $n = 20$  individuals per provenance, treatment, and time) of each trait.

toward the end of the drought stress, with provenance P2 exhibiting greater declines compared to P1 (Fig. S6). This suggests that P2 may be more sensitive to drought in terms of growth inhibition than P1.

To determine how accurately the 3D scanner-derived height represented actual seedling height, we compared it with manual stem length measurements ( $n = 80$ ). A highly significant correlation ( $R^2 = 0.94\text{--}0.96$ ,  $P < 2.2\text{e-}16$ ) confirmed the accuracy of the 3D scanning method (Fig. S7). Furthermore, we observed a moderate but significant correlation ( $R^2 = 0.65\text{--}0.76$ ,  $P < 2.2\text{e-}16$ ) between RGB-derived canopy area and 3D scanner-derived height. This indicates that while both sensors capture related aspects of growth, they provide distinct and complementary information under drought stress. Taken together, these results highlight the usefulness of RGB imaging and 3D scanning in assessing Norway spruce seedling growth and detecting provenance-specific differences in biomass allocation and vertical growth.

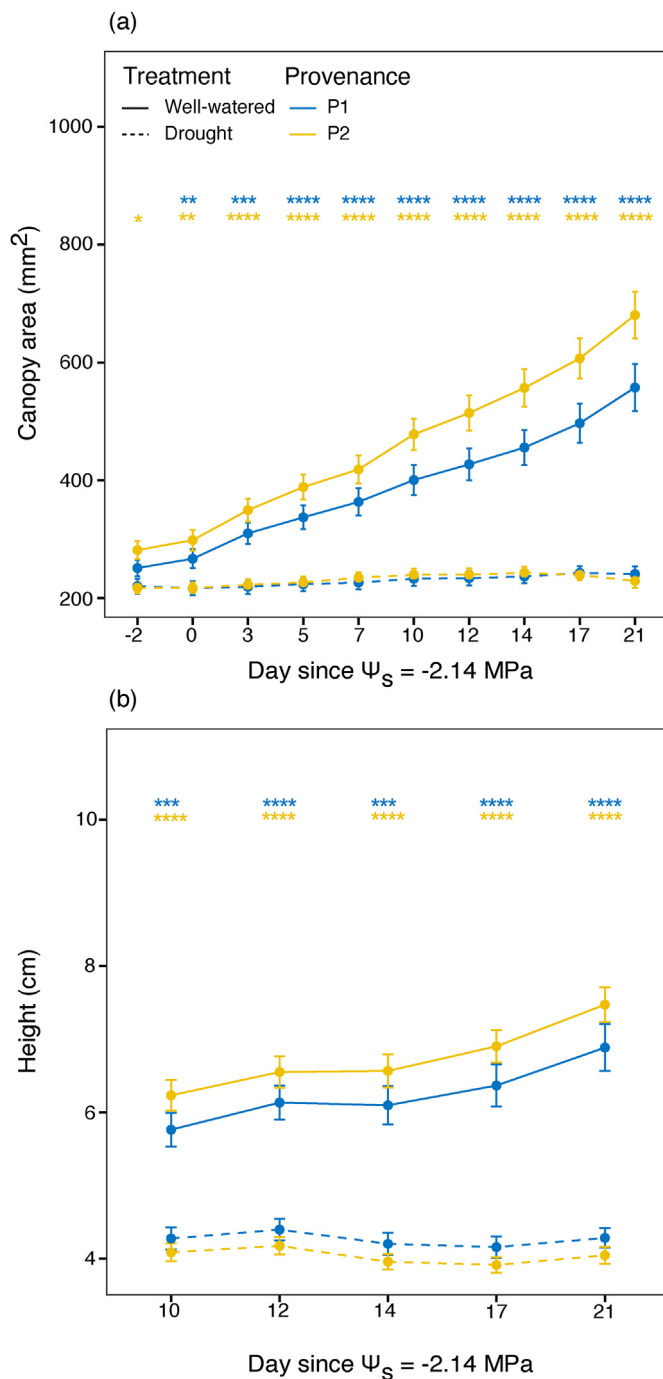


**Fig. 2.** Effect of drought stress on plant growth assessed by Red, Green, Blue (RGB), and 3D sensors. (a) Green needle area from RGB-top view. (b) Height of seedlings measured from 3D point clouds. Asterisks indicate significant differences between treatments at each time point as assessed by the non-parametric Wilcoxon test. (P-values were corrected using Bonferroni's method. \* = P.adj < 0.05; \*\* = P.adj < 0.01; \*\*\* = P.adj < 0.001). Error bars indicate the standard error of means (n = 20 biological replicates).

### 3.3. Chlorophyll fluorescence imaging reveals early and late changes in PSII performance in response to simulated drought

The decline in photosynthetic efficiency is a key indicator of drought stress, reflecting physiological basis of growth reductions captured by RGB/3D sensors. CHLF imaging revealed a significant ( $P < 0.05$ )

reduction in steady-state  $\Phi\text{PSII}_{\text{Lss}}$  and an increase in  $\text{NPQ}_{\text{Lss}}$  during the early stage of drought stress (day -2 to day 7) (Fig. 3a and b). As drought stress progressed (after day 7; referred to as the late stage),  $\Phi\text{PSII}_{\text{Lss}}$  continued to decline, while  $\text{NPQ}_{\text{Lss}}$  initially returned to well-watered levels before eventually dropping below those of non-stressed plants (Fig. 3a and b; Movie S1). Evidence of PSII damage became apparent with a significant and pronounced decline in maximum quantum yield ( $F_v/F_m$ ) during the late stage (Fig. 3c; Movie S2). This decline was accompanied by significant increase in minimal fluorescence ( $F_0$ ; Fig. 3d) and a decrease in maximal fluorescence ( $F_m$ ) (Fig. S3), indicative of photo-inhibition and inactivation of PSII centers.

In addition to these general drought responses, provenance-specific differences were observed in both the magnitude and timing of PSII changes.  $\Phi\text{PSII}_{\text{Lss}}$  declined earlier in P1, followed by an earlier activation of  $\text{NPQ}_{\text{Lss}}$  as compared to P2 (Fig. 3a and b). Moreover,  $\text{NPQ}_{\text{Lss}}$  levels during early drought stage were relatively significantly higher ( $P < 0.05$ ), suggesting that P1 responded more rapidly and strongly to drought by initiating photoprotection sooner (Fig. S6). Furthermore, towards the end of drought stress, all observed traits (except  $F_0$ ) exhibited a greater relative reduction in P2 than in P1 (Fig. S6). Although these differences did not reach significance ( $P < 0.05$ ), they hint at a tendency toward greater photosynthetic inhibition in P2, mirroring its stronger growth reduction.

Taken together, these results highlight the utility of CHLF imaging in distinguishing early and late stages of drought stress responses in Norway spruce, revealing physiological insight that extend beyond the growth measurements provided by RGB/3D sensors. By capturing biphasic nature of drought responses, CHLF imaging offers a potential physiological explanation for growth reductions and provides complementary insights into provenance specific drought sensitivity.

### 3.4. Hyperspectral imaging reveals differences in reflectance and tissue water content between treatments and provenances

Drought stress alters plant optical properties by affecting tissue water content and pigment composition. To investigate these changes, canopy reflectance signatures from 350 nm to 1700 nm were measured. Canopy reflectance showed a significant increase ( $P < 0.05$ ) in the SWIR range (~1350–1700 nm) in drought-stressed seedlings during the early stage, with P1 affected earlier than P2 (Fig. S8). This increase expanded across the entire SWIR region (900–1700 nm) during late stage, potentially reflecting plant water status. Similarly, VNIR reflectance (550–700 nm, 800–900 nm) increased under drought (Fig. S8), presumably due to pigment and structural changes. Provenance-specific differences in relative reflectance were observed between 509 and 724 nm at 17 and 21 days after drought onset (Fig. S9). While reflectance increased in both provenances, the relative increase was greater in P1 than in P2.

To quantify these spectral shifts, we calculated eight indices. The  $r_{1440}/r_{960}$  ratio, an indicator of tissue water content, increased under drought (Fig. 3e). Among seven vegetation indices, NDVI, PSRI, and SIPI showed strong significant changes towards the end of drought stress. Meanwhile, MCARI, PRI, OSAVI, and NDVI2 were overall non-significant (Fig. S10). To assess whether these indices could serve as proxies for pigments in seedlings, a correlation analysis was performed. NDVI and other indices showed significant correlations ( $P < 0.05$ ) with zeaxanthin,  $\beta$ -carotene and chlorophyll *b*. However, weak and non-significant correlations were observed for total chlorophyll or chlorophyll *a* content (Fig. S11), suggesting challenges of measuring small canopy areas as highlighted by Ref. [18].

Taken together, our results highlight the utility of hyperspectral sensors for drought monitoring and detecting provenance-specific differences but also reveal the need for methodological refinements, particularly in assessing chlorophyll content in small-canopy seedlings.

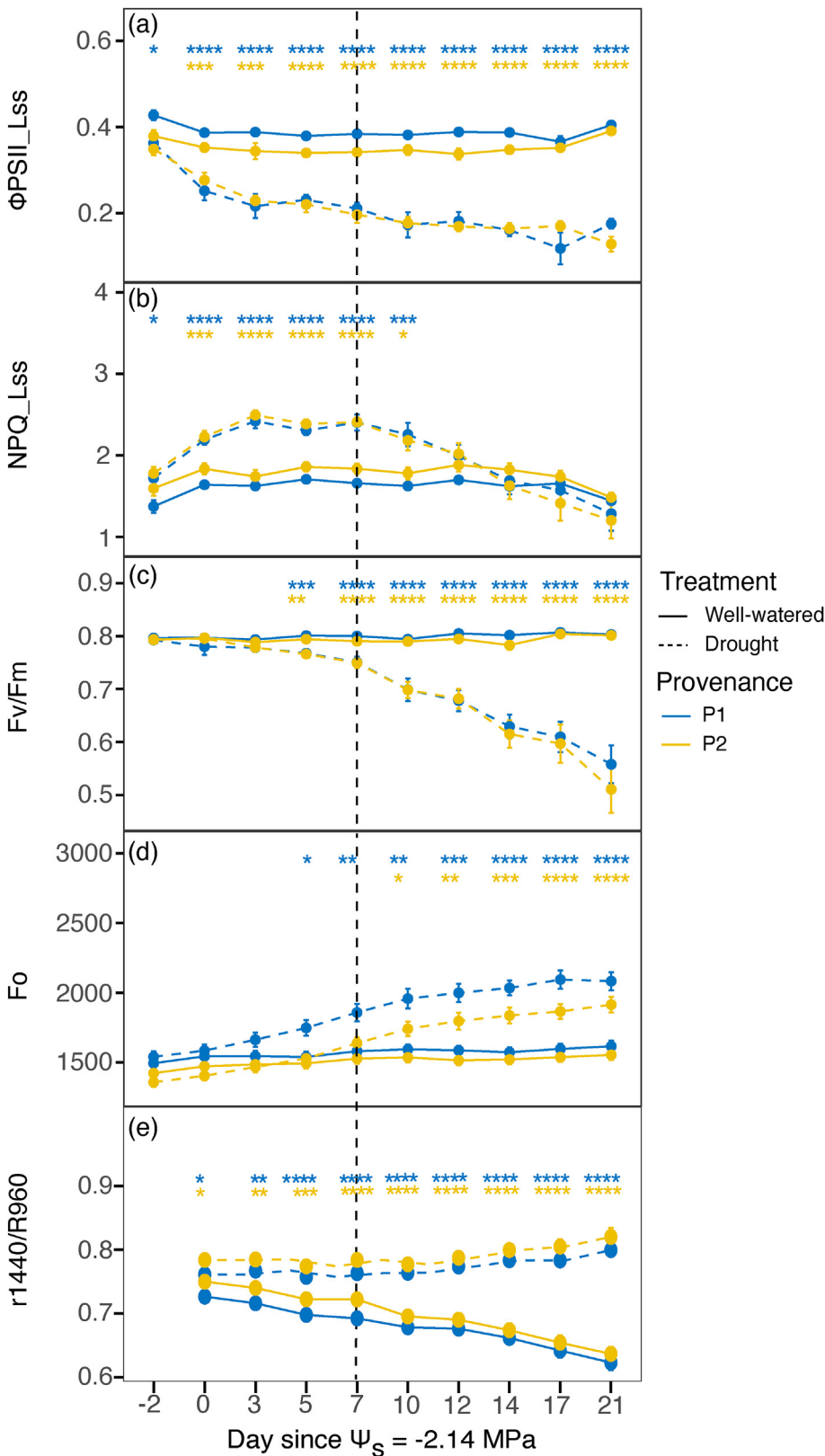


**Fig. 3.** Effect of drought stress on photosystem II (PSII) and tissue water contents of two provenances of Norway spruce seedlings assessed by pulse amplitude modulated (PAM) chlorophyll fluorescence (CHLF) imaging. (a) Steady-state operating efficiency of PSII ( $\Phi_{PSII\_Lss}$ ). (b) Steady-state non-photochemical quenching ( $NPQ\_Lss$ ) rising from day -2-7 and consequently decreasing until day 21 (c) Maximum quantum yield of PSII ( $Fv/Fm$ ) decreasing moderately until day 7 and rapidly afterward until day 21 indicating increasing photoinhibition. (d) Minimal fluorescence ( $F_0$ ) rises during drought treatment indicating increasing photoinhibition. (e) Tissue water contents evaluated using the water index ( $r_{1440/r960}$ ). Asterisks indicate significant differences between treatments at each time point as assessed by the non-parametric Wilcoxon test. (P-values were corrected using Bonferroni's method. \* = P.adj <0.05; \*\* = P.adj <0.01; \*\*\* = P.adj <0.001). Error bars indicate the standard error of means (n = 20 biological replicates).

**3.5. Drought stress triggers foliar levels of different phytohormones in a time-dependent manner in Norway spruce seedlings**

The physiological and growth responses observed under drought stress are regulated by phytohormones. To investigate which

phytohormones modulate under drought and might be involved in regulation of these responses, we measured foliar concentrations of different phytohormones during early and late stages of drought (0, 7, 14, and 21 days). Among the quantified hormones were abscisic acid (ABA), salicylic acid (SA), jasmonate (JA), indole acetic acid (IAA), gibberellins

(GA1 and GA4) and cytokinins (CKs; iP, tZ, and DHZ).

ABA levels increased significantly ( $P < 0.05$ ) in drought-stressed seedlings and peaked at day 7 in both provenances (Fig. 4a), consistent with marked reduction observed in  $\Phi$ PSII\_Lss. In addition to ABA, we observed significantly ( $P < 0.05$ ) higher accumulation of IAA and CKs in drought-stressed plants. While IAA increased later in the drought period, CKs rose early (Fig. 4b–e), suggesting their distinct roles in drought acclimation at different stages. Although non-significant, a tendency towards increased production of IAA and CKs was notable in P1, consistent with its lesser growth reduction and damage to PSII. Other hormones (SA, JA, and GAs) exhibited stochastic and provenance specific trends, with P1 generally showing greater drought-induced hormonal fluctuations than P2 (Fig. S12).

In summary, these results show that drought stress triggered distinct hormonal adjustments, linking hormonal regulation to observed phenotypic responses and explaining phenotypic differences between provenances.

### 3.6. Metabolic adjustments under drought stress in Norway Spruce

To cope with drought stress, plants produce a range of metabolites involved in NPQ (e.g., zeaxanthin and lutein) and oxidative stress mitigation (e.g., tocopherols, phenolics and terpenoids). To investigate these metabolic adjustments, we first quantified pigments (zeaxanthin, lutein, violaxanthin, neoxanthin,  $\beta$ -carotene and chlorophylls) and tocopherols at four time points (0, 7, 14, and 21 days) covering both the early and the late stages of drought.

Among pigments, zeaxanthin increased significantly ( $P < 0.05$ ) in drought-stressed seedlings of both provenances, while lutein showed a significant increase only in P2. However, its basal levels were higher in P1 (Fig. 5a; Fig. S13). Notably, zeaxanthin increased during early stage of drought and remain these levels towards the end (Fig. S13). While other pigments exhibited some modulation under drought, these changes were not significant (data not shown). Among tocopherols, only  $\alpha$ -tocopherol increased significantly ( $P < 0.05$ ) in response to drought, whereas  $\beta$ - and  $\gamma$ -tocopherols remained unchanged (Fig. 5b, Fig. S13). Importantly, the temporal dynamics of  $\alpha$ -tocopherol mirrored those of zeaxanthin, with an early increase followed by sustained elevated levels (Fig. S13).

Next, we performed untargeted metabolite profiling to assess changes in phenolics and terpenoids. While terpenoid levels remained unchanged (Fig. S14, Table S4), phenolics exhibited increased production over time. The PCA of the phenolic features ( $n = 1021$  features; Table S5) showed a clear separation of the treatments and time along the PC1 (56.6% variation), while a clear distinction between provenances could be observed along the PC2 (11.3% variation) (Fig. 6a). The total phenolic (sum of 1021 features) content increased in both provenances in response to drought stress, and these differences were significant ( $P < 0.05$ ) during late stage of drought (Fig. 6b). Furthermore, a hierarchical clustering of 43 curated phenolic metabolites revealed three metabolic clusters (Fig. 6c–Table S6). The first cluster, which contains acylated flavonols, hydroxybenzoic acid conjugates, and hydroxycinnamic acid derivatives, increased under drought stress. The second cluster, which contains glycosylated flavonols, flavones, and stilbenes, were abundant in P2 (irrespective of the treatment). The third cluster contains lignin precursors (e.g., coniferyl alcohol, sinapaldehyde glucoside, and sinapoyl glucose) that decreased upon drought stress. Taken together, these findings suggest that Norway spruce employ multilayer metabolites to cope with different stages of drought stress.

### 3.7. Drought stress reprograms the transcriptome of Norway spruce seedlings

To investigate the molecular basis of underlying drought stress responses, we performed a comparative transcriptome analysis on foliar tissues collected at day 14, when strong phenotypic and metabolic shifts were observed. PCA of gene expression profiles revealed a clear

separation between well-watered and drought-stressed samples along PC1 (95% variation), indicating a strong transcriptional shift under drought. Meanwhile, provenance-specific differences under drought were captured along PC2 (2% variation) (Fig. 6d). A total of 4671 (P1) and 4963 (P2) differentially expressed genes (DEGs) were identified in response to drought stress, with most being shared between provenances (Fig. 6e). However, a subset of genes showed provenance-specific expression, with 1173 (P1) and 1465 (P2) DEGs uniquely regulated (Fig. 6e; Data S1). The higher number of DEGs in P2 suggest it is higher susceptibility to drought aligning with trends observed in the phenotypic data.

To assess the biological significance of DEGs, we performed GO term enrichment analysis ( $P < 0.01$ ). Upregulated genes were enriched for abiotic stress responses, including water deficit, oxidative stress, and ABA signaling (Fig. S15, Data S2-3), consistent with increased ABA levels. In contrast, downregulated genes were associated with photosynthesis, ATP biosynthesis, and nucleotide metabolism (Fig. S15). A closer look at the photosynthesis-related genes revealed that the majority of the photosynthetic machinery was heavily downregulated (Fig. 6f), aligning with the observed decline in growth and PSII efficiency. Notably, the D1 repair protein was significantly downregulated only in P2, indicating a reduced capacity for PSII repair in this provenance compared to P1.

While GO enrichment identified broad biological processes affected by drought, KEGG analysis provided additional insights into specific metabolic pathways involved in drought stress. Importantly, genes related to plant hormone signaling (Fig. 6f), flavonoid and phenylpropanoid metabolism were differentially expressed, suggesting their roles in regulating stress signaling, and secondary metabolism (Table S7).

Overall, these transcriptomic shifts highlight a strong molecular response to drought, underpinning physiological, hormonal, and metabolic adjustments in Norway spruce seedlings.

### 3.8. Drought stress reduces growth and formation of stem tissues in Norway spruce seedlings

Stem anatomical traits are commonly employed in tree seedlings to assess hydraulic efficiency [30], providing insights into structural changes under drought. To investigate these changes, we measured anatomical traits in both provenances at the final time point. Under well-watered conditions, the two provenances did not significantly differ in their stem anatomy, although P2 tended to have a higher stem radius, a higher proportion of xylem, and a lower proportion of phloem (not significant; Table 1).

Drought significantly ( $P < 0.05$ ) impacted hydraulic function by reducing stem radius by 35%, primarily due to a 52% reduction in phloem, 41% in xylem, and 20% in bark (Table 1). The greater reduction in phloem than xylem resulted in a lower phloem-to-xylem ratio under drought, suggesting a shift in carbon allocation towards water transport over sugar transport (Table 1). When comparing provenances, P2 showed a slightly stronger reduction in majority of tissues, leading to more pronounced shifts in tissue distribution under drought (Table 1). Although non-significant, these trends point towards higher susceptibility of P2 aligning with patterns observed in HTPP data.

To investigate whether HTPP-derived traits can serve as proxies for these labour-intensive anatomical measurements, we examined their relationship with anatomical traits. RGB-derived traits exhibited the strongest and significant ( $P < 0.05$ ) overall correlations with anatomical traits (xylem and number of tracheids). However, under drought conditions, the correlations for P1 were weak and non-significant relative to those for P2 (Fig. S16), suggesting decoupled growth dynamics across tissue layers in P1 and a need for provenance-treatment specific models to predict anatomical traits.

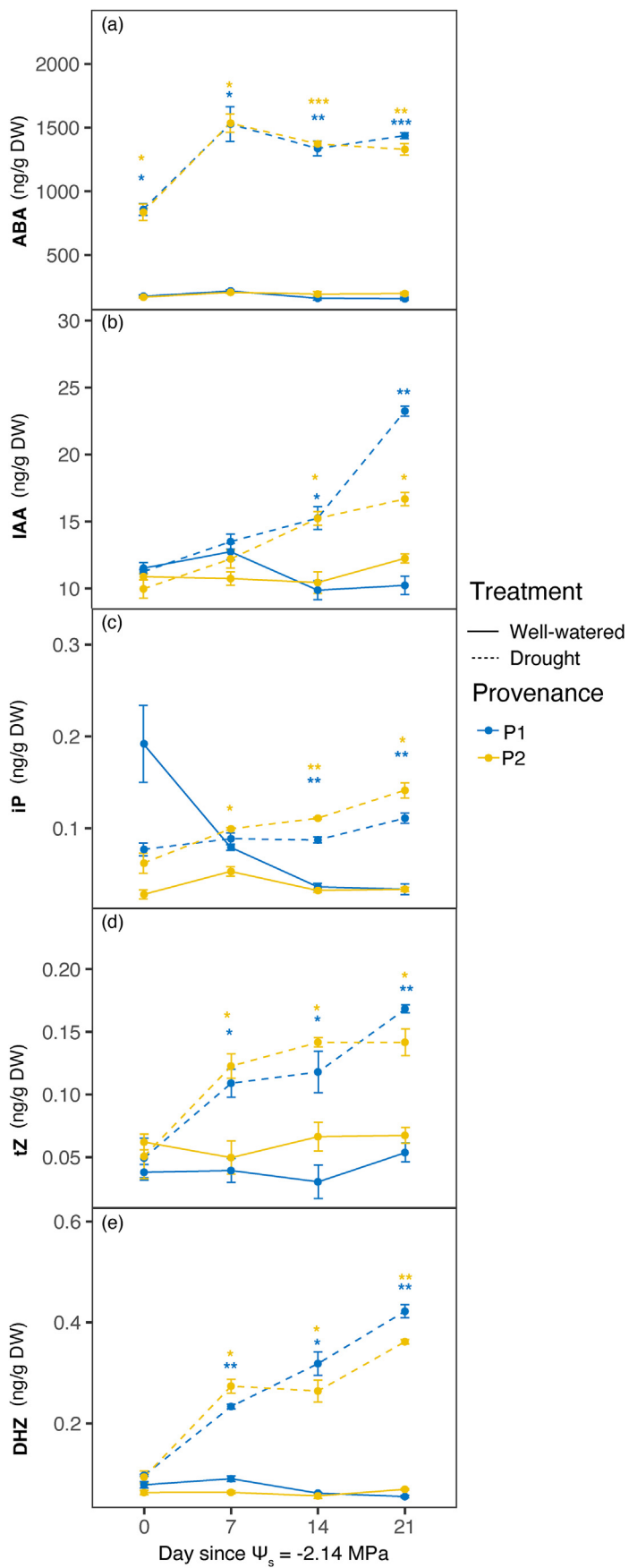


**Fig. 4.** Effect of drought stress on shoot phytohormones profiles of two provenances of Norway spruce. (a) Abscisic acid (ABA) (b) Indole acetic acid (IAA). (c) Isopentenyladenine (iP). (d) *trans*-zeatin (tZ). (e) Dihydrozeatin (DHZ). Asterisks indicate significant differences between treatments at respective time points assessed by *t*-test. (P-values were corrected using the FDR method. \* = P.adj < 0.05; \*\* = P.adj < 0.01; \*\*\* = P.adj < 0.001). Error bars indicate standard error of means. (n = 3 technical replicates derived from the pool of 19–24 individual/provenance/treatment/time point).

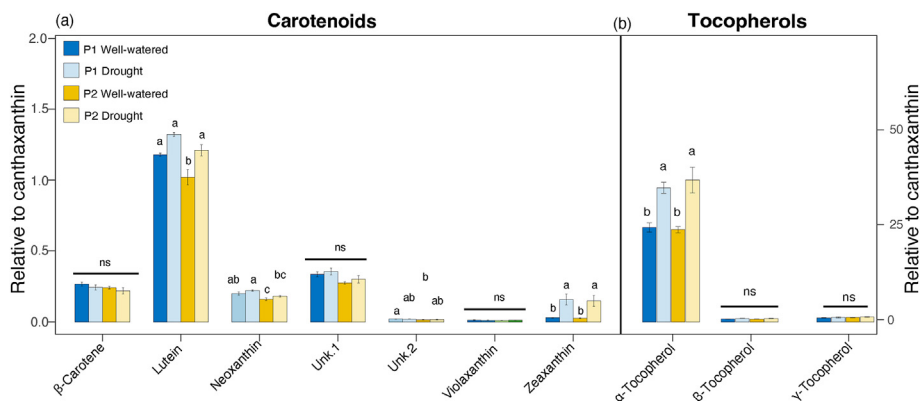


**Fig. 5.** Effect of drought stress on shoot carotenoid and tocopherol profiles of two provenances of Norway spruce. (a) Carotenoids profiles. (b) Tocopherols. Each bar plot represents the average of four replicates where each replicate depicts a pooled sample from 0, 7, 14, and 21 days after target  $\Psi_s$  reached. Different letters denote statistically significant differences for each compound between treatments and provenances tested by two-way ANOVA followed by the Tukey HSD test. Error bars indicate the standard error of means. ( $n = 4$  replicates collected from four different time points).

#### 4. Discussion

Drought stress poses a significant threat to Norway spruce productivity, affecting both survival and growth [2,5,6]. Understanding the physiological and molecular basis underlying drought responses is essential for developing adaptive forest management strategies. While previous studies have examined drought responses in Norway spruce [8, 12], they often relied on labor intensive measurements or end-point assessments, limiting insight into dynamic stress responses and constraining large-scale screening. Here, we show an example of how HTPP enables non-invasive detection and tracking of different drought stages while also offering the potential to screen large number of provenances efficiently. The combination of different sensors was crucial to capture the dynamic nature of drought responses. By integrating metabolomics and transcriptomics with HTPP, we further show that Norway spruce employ multi-layer metabolic adjustments as seedlings transition from acclimation (early stage responses e.g., photoprotection) to damage (late stage responses e.g., damage to PSII). This highlights the synergistic potential of HTPP and omics integration for assessing drought stress responses in Norway spruce seedlings.

##### 4.1. Photoprotection in action during the early stage of drought stress in Norway spruce seedlings

In plants, stomatal closure is a key early drought response that conserves water but also limits  $\text{CO}_2$  uptake, constraining photosynthesis [31, 32]. As an isohydric species, Norway spruce relies primarily on ABA-mediated stomatal closure to maintain constant xylem water potential and delay hydraulic failure [33]. Consistent with this strategy, we observed halted growth and reduced photochemical efficiency ( $\Phi\text{PSII}_{\text{Lss}}$ ) during the early drought stage, indicating a shift toward resource conservation. This response was accompanied by a significant early accumulation of ABA and upregulation of its biosynthetic and signaling genes, aligning with its role in stomatal regulation and stress signaling [34]. Despite lower water content, its stability in the early phase suggests that ABA-induced stomatal closure effectively minimized further water loss, likely buffering the onset of hydraulic failure.

Although stomatal closure reduces transpiration, it also increases the risk of photooxidative stress by limiting  $\text{CO}_2$  availability for photochemistry, causing excess excitation energy to accumulate in PSII [35]. As an adaptation, plants generally activate photoprotection via NPQ\_LSS to dissipate extra excitation energy as heat [36,37]. Xanthophyll pigments such as lutein and zeaxanthin have been shown to play an indispensable role in such photoprotective mechanisms [36,37]. During initial drought phase, NPQ\_Lss indeed increased significantly, accompanied by elevated zeaxanthin and lutein levels, indicating a rapid photoprotective response. The minor signs of PSII damage indicated by Fv/Fm, higher levels of NPQ\_Lss, and xanthophylls imply that during the initial phase, photoprotection kept at pace in circumventing deleterious effects of

overexcitation of PSII.

In addition to NPQ-dependent photoprotection, tocopherols and CKs may have provided additional protection to PSII. Tocopherols function as key antioxidants, preventing lipid peroxidation and scavenging reactive oxygen species (ROS) to maintain thylakoid membrane stability [38]. Meanwhile, CKs, although primarily known for their role in growth regulation, also contribute to stress tolerance by preserving photosynthetic efficiency, delaying senescence, and mitigating oxidative damage [39–41]. Furthermore, increased CK levels in Norway spruce have been potentially linked to enhanced drought adaptation [42]. The observed increase in tocopherols and CKs during the early stage in our study thus suggests a protective mechanism against PSII damage. Collectively, these findings indicate a multilayered protective strategy in Norway spruce seedlings, where NPQ\_Lss, ABA, CKs, and tocopherols act in concert to regulate water loss, maintain photosynthetic function, and mitigate oxidative stress during early drought acclimation.

While these responses in Norway spruce have been previously studied [42,43], they have not been assessed in an integrated, non-invasive manner. By combining HTPP-derived traits with metabolomics, our study reveals the synergy between growth, physiological, and metabolic responses driving early acclimation in Norway spruce. This integration uncovered coordinated interactions between growth, stomatal regulation, NPQ, metabolic shifts, and tissue water dynamics—insights that may be missed when studied in isolation. It further provides a comprehensive framework to understand how Norway spruce acclimates to short-term drought across multiple functional levels. Future research using more contrasting provenances could clarify how early stage traits, particularly NPQ\_Lss, contribute to drought adaptation, refining selection strategies for tolerant provenances.

##### 4.2. Extended exposure to drought stress extensively damages the photosystem of Norway spruce seedlings

As drought stress persists, plants shift from acclimation to damage, with increasing impairment of photosynthesis and photoprotection [44, 45]. In our study, this transition became evident after day 7, when  $\Phi\text{PSII}_{\text{Lss}}$  reached its minimum while NPQ\_Lss progressively declined to well-watered levels. The weakening of NPQ\_Lss suggests that photoprotective energy dissipation was insufficient, increasing the risk of oxidative stress and photoinhibition (light-induced damage of PSII) [46]. Excess energy in PSII intensifies ROS production and promotes chlorophyll triplet state formation, leading to oxidative damage and PSII instability [47]. In line with this, the decline in Fv/Fm and rise in Fo indicate sustained photoinhibition [48]. Meanwhile, enhanced non-regulated energy dissipation (Fig. S17) suggests a high ROS burden [49,50], likely surpassing the scavenging capacity of the observed protective responses. The repression of psbA (D1 protein) further supports this excessive strain on PSII, as sustained damage requires continuous D1 degradation and resynthesis to maintain photochemical efficiency [46].

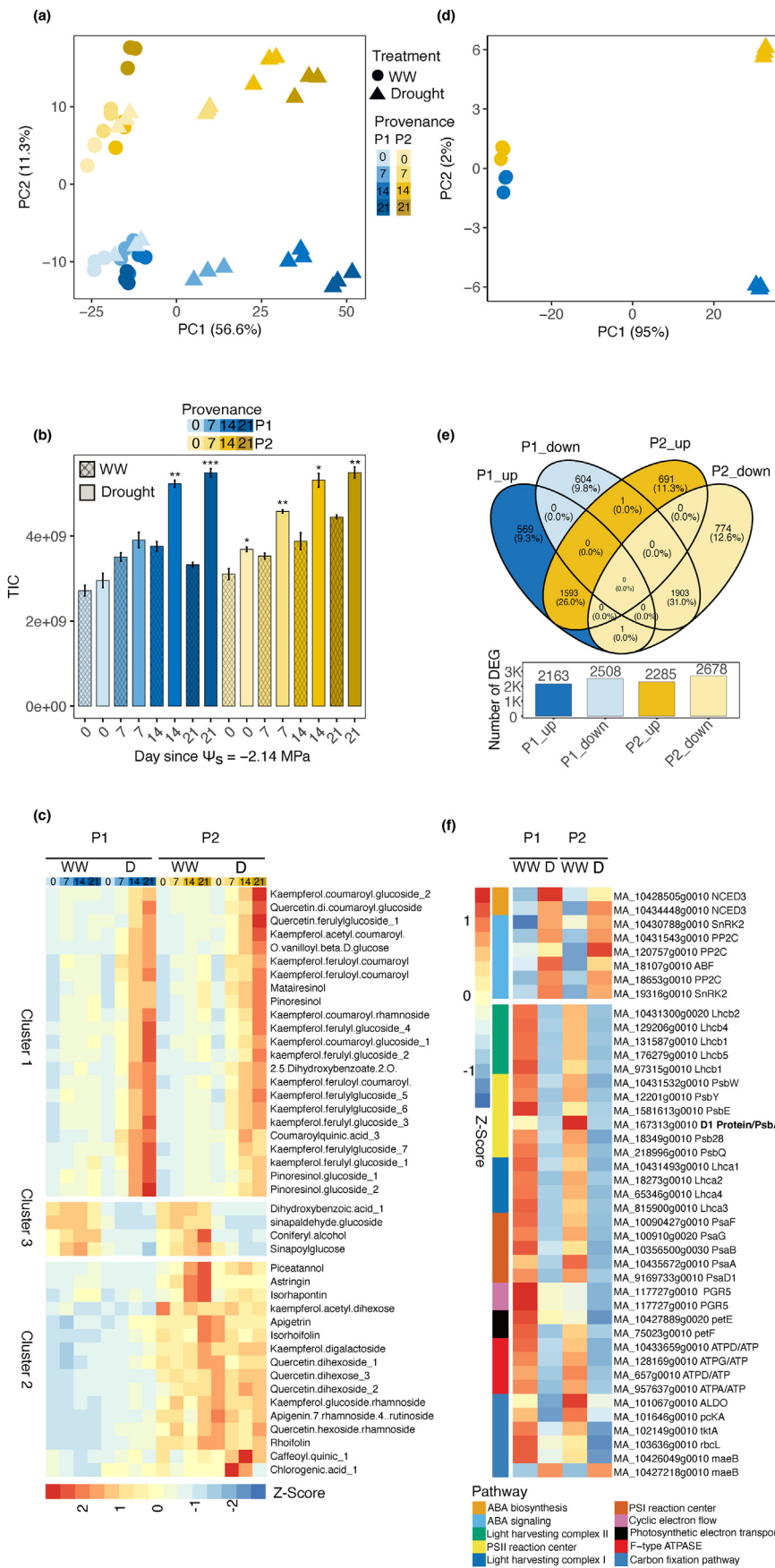


**Fig. 6.** Effect of drought stress on shoot phenolics and transcriptome profiles of two provenances of Norway spruce. (a) Principal component analysis (PCA) of metabolic profiles of studied provenances at different time points. Note the differences between treatments and time along PC1 and provenance differences on PC2. (b) Total phenolics (sum of 1021 features) contents in well-watered (WW) and drought-stressed (D) samples at four different time points. Asterisks indicate significant differences between treatments at respective time points assessed by *t*-test. P-values \* =  $P < 0.05$ ; \*\* =  $P < 0.01$ ; \*\*\* =  $P < 0.001$ . Error bars indicate the standard error of means. ( $n = 3$  technical replicates derived from the pool of 19–24 individuals per provenance, treatment, and time point). (c) Hierarchical cluster analysis of identified and annotated 43 phenolics compounds. (d) PCA of transcript profiles. (e) Venn diagram exhibits the number of shared and unique differentially expressed genes (DEG) (FDR  $< 0.05$ ) between provenances. The bar plots below the Venn diagram represent number of up-and downregulated DEG in each provenance with respect to well-watered seedlings. (f) Heatmap of DEG of ABA biosynthesis, signaling and photosynthesis pathways. The bold letters indicate significance for D1 exclusively in P2. For clarity only a subset of genes is shown from these pathways. A complete list is provided in Table S7.

**Table 1**

Stem anatomical traits measured (mean  $\pm$  se) for control and drought-stressed individuals from both provenances at the last time point (21 days after the onset of drought stress). Different letters indicate significant differences between the groups.

	Control		Drought		Relative Reduction (%)	
	P1	P2	P1	P2	P1	P2
Stem radius ( $\mu\text{m}$ )	493.55 $\pm$ 16.61 <sup>a</sup>	508.75 $\pm$ 23.52 <sup>a</sup>	330.63 $\pm$ 8.37 <sup>b</sup>	327.19 $\pm$ 9.34 <sup>b</sup>	-33.00	-35.70
Pith width ( $\mu\text{m}$ )	59.70 $\pm$ 4.20 <sup>a</sup>	53.79 $\pm$ 4.78 <sup>ab</sup>	43.19 $\pm$ 1.37 <sup>b</sup>	47.41 $\pm$ 2.28 <sup>ab</sup>	-27.70	-11.90
Xylem width ( $\mu\text{m}$ )	223.47 $\pm$ 11.78 <sup>a</sup>	245.02 $\pm$ 15.35 <sup>a</sup>	136.67 $\pm$ 5.09 <sup>b</sup>	134.55 $\pm$ 5.92 <sup>b</sup>	-38.80	-45.10
Phloem width ( $\mu\text{m}$ )	69.84 $\pm$ 4.79 <sup>a</sup>	66.00 $\pm$ 5.64 <sup>a</sup>	33.91 $\pm$ 2.61 <sup>b</sup>	30.37 $\pm$ 2.16 <sup>b</sup>	-51.40	-54.00
Bark width ( $\mu\text{m}$ )	123.33 $\pm$ 4.25 <sup>a</sup>	126.28 $\pm$ 7.40 <sup>a</sup>	100.75 $\pm$ 5.94 <sup>b</sup>	99.22 $\pm$ 5.00 <sup>b</sup>	-18.30	-21.40
Epidermis width ( $\mu\text{m}$ )	17.21 $\pm$ 0.73	17.65 $\pm$ 0.50	16.11 $\pm$ 0.67	15.64 $\pm$ 0.58	-6.40	-11.40
n tracheids	17.58 $\pm$ 0.92 <sup>a</sup>	18.75 $\pm$ 0.94 <sup>a</sup>	11.75 $\pm$ 0.43 <sup>b</sup>	11.25 $\pm$ 0.41 <sup>b</sup>	-33.20	-40.00
d tracheids ( $\mu\text{m}$ )	12.74 $\pm$ 0.21 <sup>a</sup>	12.98 $\pm$ 0.23 <sup>a</sup>	11.65 $\pm$ 0.22 <sup>b</sup>	11.95 $\pm$ 0.25 <sup>b</sup>	-8.54	-7.92
Phloem/xylem ratio	0.32 $\pm$ 0.02 <sup>a</sup>	0.27 $\pm$ 0.02 <sup>ab</sup>	0.25 $\pm$ 0.02 <sup>ab</sup>	0.23 $\pm$ 0.02 <sup>b</sup>	-20.40	-14.90

Beyond psbA, our transcriptional data also revealed widespread repression of genes encoding PSI/PSII core proteins, light harvesting complexes, electron transport components, and F-type ATP synthase. Together, these molecular responses indicate severe photoinhibition, disrupted electron transport, and energy depletion, ultimately constraining photosynthetic capacity and limiting the plant's ability to sustain metabolic homeostasis under prolonged drought stress. Interestingly, at the end of the drought phase, IAA production was boosted suggesting the initiation of investment in root development and further highlighting that the last strategy employed by the plants to cope with drought stress [51].

With photoprotective and PSII repair mechanisms weakening, plants increasingly rely on additional antioxidant defenses to overcome ROS accumulation [46]. In addition to xanthophylls and tocopherols, phenolics are well-established ROS scavengers, often accumulating under different stress conditions to mitigate oxidative damage and have been linked to drought tolerance in different plant species [52–54]. However, their role in Norway spruce remains unclear, with reports of both increased and decreased phenolic levels under drought [55–58]. In our study, phenolics increased significantly during late drought stress, coinciding with reduced NPQ and enhanced non-regulated energy dissipation, suggesting a compensatory response to high oxidative stress. However, despite increased phenolic accumulation, severe impairment of the photosystem was evident at both the transcriptional level, with downregulation of key photosynthetic genes, and the functional level, as reflected by the decline in Fv/Fm. This suggests that phenolics alone might have been insufficient to fully prevent damage to photosystem and may act as a secondary, compensatory defense rather than a primary protective mechanism. This hypothesis is further supported by the lack of a clear protective advantage in P2, which constitutively exhibited higher phenolic levels yet experienced greater photosynthetic and growth reduction under drought. Alternatively, it might be possible that induced phenolics levels or higher constitutive levels in P2 are still lower than what might be required to mitigate oxidative stress under prolonged drought. Future studies incorporating provenances with varying phenolic levels and drought intensities are needed to confirm these hypotheses.

While these findings reveal a critical transition in Norway spruce from early acclimation to late-stage damage, they also highlight the potential of late stage traits as indicators of long-term drought tolerance. Although most studies in Norway spruce focus on growth and survival, we propose that integrating both early (NPQ,  $\Phi\text{PSII}$ , Lss, tissue water content, growth) and late stage traits (Fv/Fm, Fo) with omics approaches would provide a more comprehensive framework for evaluating drought tolerance. This approach not only differentiates transient acclimation from progressive stress-induced damage but also captures key metabolic and molecular adjustments, facilitating the identification of molecular targets for enhancing drought tolerance.

## 5. Conclusions

In summary, we have developed a comprehensive HTPP protocol for

precise, accurate, and non-invasive monitoring of the physiological and growth status of Norway spruce under drought stress. By integrating this technique with metabolomics, transcriptomics, and anatomy, we provide a detailed insight into how two provenances of Norway spruce seedlings cope with drought stress. Through this approach, we highlight key phenotypic traits that distinguish early-phase acclimation (e.g., growth, tissue water content,  $\Phi\text{PSII}$ , NPQ) from late-stage drought damage (e.g., Fo, Fv/Fm) and provenance-specific differences (e.g., Fp). The recovery of similar drought stress response patterns across datasets (Fig. S18) in two independent provenances highlights the robustness of the established method. Meanwhile finding provenance-specific differences from narrow geographic distribution suggests higher potential and sensitivity of the method to screen adaptive variation. Overall, our work has laid the groundwork for a rapid assessment that will aid forest biotechnology researchers and breeders in determining the most suitable and resilient forest reproductive material for drought-prone conditions. This information will be vital for effective forest management in the coming years, as climate change is predicted to bring about heightened drought occurrences.

## Author contributions

CTM conceived the project concept. MA, MvL, and CTM designed the research. MA and EG performed the experiment. JJ and SS performed the phenotyping. AG and SM performed anatomical analysis. RU performed data extraction from 3D point clouds and wrote Python scripts for KEGG analysis. AER, EC, MAM-G, and JB performed all of the metabolite analyses. CP contributed to fluorescence and metabolite data interpretation. MA analyzed all the datasets and prepared the first draft of the manuscript. CTM and MvL supervised the research. All authors read, reviewed, and edited the manuscript.

## Data availability

The RNA-seq data has been uploaded to NCBI under the accession number PRJNA1043659.

## Declaration of generative AI and AI-assisted technologies in the writing process

During the preparation of this work the author(s) used chatgpt in order to improve the language and grammar of the manuscript. After using this tool, the author(s) reviewed and edited the content as needed and take(s) full responsibility for the content of the publication.

## Funding

Financial support was provided by the Austrian Research Promotion Agency (FFG) and grant Nu. 2021–0.382.292 (project: climate smart forests: provenance selection and planting method\_AP2) with funds from the departmental research program through dafne.at with resources from

the Federal Ministry of Agriculture, Regions, and Water Management. The Federal Ministry supports applied, problem-oriented, and practice-oriented research within the competence area of the department. We acknowledge The Austrian Research Promotion Agency (FFG) - R&D Infrastructure Funding Programme - PHENOPlant project #870446" for the PHENOPlant research infrastructure. The Vienna BioCenter Core Facilities (VBCF) Plant Sciences Facility acknowledges funding from the Austrian Federal Ministry of Education, Science & Research; and the City of Vienna. Further support was provided by the Austrian Science Funds FWF, projects P32203-B "Legacy effects after summer and winter drought" and DOC 171 "The future of mountain forests".

### Declaration of competing interest

The authors declare that they have no known competing financial interests or personal relationships that could have appeared to influence the work reported in this paper.

### Acknowledgments

We thank Michaela Breuer, and Florence Lee for their assistance in setting up the experiment, Richarda Schuller for seed germination assay, Georg Mairhofer for help with stem anatomical measurements, Dagamar Topola for providing seeds of Norway spruce, Anneliese Auer and Paula Helfenbein for the technical support with phenotyping. We thank Maria Teresa Caballero for her assistance in metabolomic sample processing and analysis. We thank Ethan Stewart for performing image segmentation and analysis. We also thank the soil physical lab of the Institute for Land and Water Management Research in Petzenkirchen, Austria for determining soil water retention curve.

### Appendix A. Supplementary data

Supplementary data to this article can be found online at <https://doi.org/10.1016/j.plaphe.2025.100037>.

### References

- [1] C. Senf, A. Buras, C.S. Zang, A. Rammig, R. Seidl, Excess forest mortality is consistently linked to drought across Europe, *Nat. Commun.* 11 (2020) 6200.
- [2] J. Aldea, R. Ruiz-Peinado, M. del Río, H. Pretzsch, M. Heym, G. Brazaitis, A. Jansons, M. Metslaid, I. Barbeito, K. Bielak, et al., Timing and duration of drought modulate tree growth response in pure and mixed stands of Scots pine and Norway spruce, *J. Ecol.* 110 (2022) 2673–2683.
- [3] J. Spinoni, J.V. Vogt, G. Naumann, P. Barbosa, A. Dosio, Will drought events become more frequent and severe in Europe? *Int. J. Climatol.* 38 (2018) 1718–1736.
- [4] A. Buras, A. Rammig, S. Zang, C. Quantifying impacts of the 2018 drought on European ecosystems in comparison to 2003, *Biogeosciences* 17 (2020) 1655–1672.
- [5] D. Chakraborty, N. Mócziz, E. Rasztovtis, L. Dobor, S. Schueler, Provisioning forest and conservation science with high-resolution maps of potential distribution of major European tree species under climate change, *Ann. For. Sci.* 78 (2021) 1–18.
- [6] H. Pretzsch, T. Grams, K.H. Häberle, K. Pritsch, T. Bauerle, T. Rötzer, Growth and mortality of Norway spruce and European beech in monospecific and mixed-species stands under natural episodic and experimentally extended drought. Results of the KROOF throughfall exclusion experiment, *Trees Struct. Funct.* 34 (2020) 957–970.
- [7] C. Zang, H. Pretzsch, A. Rothe, Size-dependent responses to summer drought in Scots pine, Norway spruce and common oak, *Trees Struct. Funct.* 26 (2012) 557–569.
- [8] J. Modrzyński, G. Eriksson, Response of *Picea abies* populations from elevational transects in the Polish Sudety and Carpathian mountains to simulated drought stress, *For. Ecol. Manag.* 165 (2002) 105–116.
- [9] W. Oberhuber, A. Hammerle, W. Kofler, Tree water status and growth of saplings and mature Norway spruce (*Picea abies*) at a dry distribution limit, *Front. Plant Sci.* 6 (2015) 703.
- [10] L. Bian, H. Zhang, Y. Ge, J. Čepel, J. Stejskal, Y.A. El-Kassaby, Closing the gap between phenotyping and genotyping: review of advanced, image-based phenotyping technologies in forestry, *Ann. For. Sci.* 79 (2022) 1–21.
- [11] N. Kunert, P. Hajek, P. Hietz, H. Morris, S. Rosner, D. Tholen, Summer temperatures reach the thermal tolerance threshold of photosynthetic decline in temperate conifers, *Plant Biol.* 24 (2022) 1254–1261.
- [12] H. Húdoková, P. Fleischer, M. Ježík, J. Marešová, E. Pšidová, M. Mukarram, Ditmarová, A. Sliacka-Konópková, G. Jamnická, Can seedlings of Norway spruce (*Picea abies* L. H. Karst.) populations withstand changed climate conditions? *Photosynthetica* 61 (2023) 328.
- [13] P. Petrik, A. Petek-Petrik, A. Konópková, P. Fleischer, S. Stojnic, I. Zavadilova, D. Kurjak, Seasonality of PSII thermostability and water use efficiency of in situ mountainous Norway spruce (*Picea abies*), *J. For. Res.* 34 (2023) 197–208.
- [14] J.L. Araus, S.C. Kefauver, M. Zaman-Allah, M.S. Olsen, J.E. Cairns, Translating high-throughput phenotyping into genetic gain, *Trends Plant Sci.* 23 (2018) 451–466.
- [15] L. Xiang, T.M. Nolan, Y. Bao, M. Elmore, T. Tuel, J. Gai, D. Shah, P. Wang, N.M. Huser, A.M. Hurd, et al., Robotic Assay for Drought (RoAD): an automated phenotyping system for brassinosteroid and drought responses, *Plant J.* 107 (2021) 1837–1853.
- [16] H. Li, W. Yang, J. Lei, J. She, X. Zhou, Estimation of leaf water content from hyperspectral data of different plant species by using three new spectral absorption indices, *PLoS One* 16 (2021) 1–16.
- [17] J. Hejtmanek, J. Stejskal, J. Čepel, Z. Lhotáková, J. Korecký, A. Krejzková, J. Dvořák, S.A. Gezan, Revealing the complex relationship among hyperspectral reflectance, photosynthetic pigments, and growth in Norway spruce ecotypes, *Front. Plant Sci.* 13 (2022).
- [18] Y. Lai, X. Mu, Y. Bian, X. Dong, F. Qiu, X. Bo, Z. Zhang, Y. Li, X. Liu, L. Li, et al., Bidirectional reflectance factor measurement of conifer needles with microscopic spectroscopy imaging, *Agric. For. Meteorol.* 330 (2023) 109311.
- [19] K.B. Katuwal, H. Yang, B. Huang, K.B. Katuwal, H. Yang, B. Huang, Evaluation of phenotypic and photosynthetic indices to detect water stress in perennial grass species using hyperspectral, multispectral and chlorophyll fluorescence imaging, *Grass.Res.* 1 (16) (2023) 3, 2023.
- [20] M. Zagorščak, L. Abdelhakim, N.Y. Rodriguez-Granados, J. Široká, A. Ghatak, C. Bleker, A. Blejec, J. Zrimec, O. Novák, A. Pěnčík, et al., Integration of multi-omics data and deep phenotyping of potato enables novel insights into single- and combined abiotic stress responses, *bioRxiv: 2024.07.18.604140* (2025).
- [21] B. Li, L. Chen, W. Sun, D. Wu, M. Wang, Y. Yu, G. Chen, W. Yang, Z. Lin, X. Zhang, et al., Phenomics-based GWAS analysis reveals the genetic architecture for drought resistance in cotton, *Plant Biotechnol. J.* 18 (2020) 2533–2544.
- [22] M. Awlia, N. Alshareef, N. Saber, A. Korte, H. Oakey, K. Panzarová, M. Trtílek, S. Negrão, M. Tester, M.M. Julkowska, Genetic mapping of the early responses to salt stress in *Arabidopsis thaliana*, *Plant J.* 107 (2021) 544–563.
- [23] P. D'Odorico, A. Besik, C.Y.S. Wong, N. Isabel, I. Ensminger, High-throughput drone-based remote sensing reliably tracks phenology in thousands of conifer seedlings, *New Phytol.* 226 (2020) 1667–1681.
- [24] A. Mazis, S. Das Choudhury, P.B. Morgan, V. Stoerger, J. Hiller, Y. Ge, T. Awada, Application of high-throughput plant phenotyping for assessing biophysical traits and drought response in two oak species under controlled environment, *For. Ecol. Manag.* 465 (2020) 118101.
- [25] F. Santini, S.C. Kefauver, J.L. Araus, V. Resco de Dios, S. Martín García, D. Grivet, J. Voltas, Bridging the genotype–phenotype gap for a Mediterranean pine by semi-automatic crown identification and multispectral imagery, *New Phytol.* 229 (2021) 245–258.
- [26] M. Sorrentino, K. Panzarová, I. Spyroglou, L. Spíchal, V. Buffagni, P. Ganugi, Y. Rouphael, G. Colla, L. Lucini, N. De Diego, Integration of phenomics and metabolomics datasets reveals different mode of action of biostimulants based on protein hydrolysates in *Lactuca sativa* L. And *Solanum lycopersicum* L. Under salinity, *Front. Plant Sci.* 12 (2022) 3333.
- [27] U. Schindler, W. Durner, G. von Unold, L. Müller, Evaporation method for measuring unsaturated hydraulic properties of soils: extending the measurement range, *Soil Sci. Soc. Am. J.* 74 (4) (2010) 1071–1083.
- [28] M. Awlia, A. Nigro, J. Fajkus, S.M. Schmoedel, S. Negrão, D. Santelia, M. Trtílek, M. Tester, M.M. Julkowska, K. Panzarová, High-throughput non-destructive phenotyping of traits that contribute to salinity tolerance in *Arabidopsis thaliana*, *Front. Plant Sci.* 7 (2016) 1414.
- [29] B. Turc, S. Sahay, J. Haupt, T. de Oliveira Santos, G. Bai, K. Glowacka, Up-regulation of non-photochemical quenching improves water use efficiency and reduces whole-plant water consumption under drought in *Nicotiana tabacum*, *J. Exp. Bot.* 75 (2024) 3959–3972.
- [30] M.L. Miller, A.B. Roddy, C.R. Brodersen, A.J. McElrone, D.M. Johnson, Anatomical and hydraulic responses to desiccation in emergent conifer seedlings, *Am. J. Bot.* 107 (2020) 1177–1188.
- [31] T. Lawson, S. Violet-Chabrand, Speedy stomata, photosynthesis and plant water use efficiency, *New Phytol.* 221 (2019) 93–98.
- [32] T. Lawson, A.D.B. Leakey, Stomata: custodians of leaf gaseous exchange, *J. Exp. Bot.* 75 (2024) 6677–6682.
- [33] E. Moran, J. Lauder, C. Musser, A. Stathos, M. Shu, The genetics of drought tolerance in conifers, *New Phytol.* 216 (2017) 1034–1048.
- [34] S. Munemasa, F. Hauser, J. Park, R. Waadt, B. Brandt, J.I. Schroeder, Mechanisms of abscisic acid-mediated control of stomatal aperture, *Curr. Opin. Plant Biol.* 28 (2015) 154–162.
- [35] J. Moustaka, I. Sperdoui, S. İşğören, B. Şaş, M. Moustakas, Deciphering the mechanism of melatonin-induced enhancement of photosystem II function in moderate drought-stressed oregano plants, *Plants* 13 (2024) 2590.
- [36] R. Bassi, L. Dall'Osto, Dissipation of light energy absorbed in excess: the molecular mechanisms, *Annu. Rev. Plant Biol.* 72 (2021) 47–76.
- [37] S.P. Long, S.H. Taylor, S.J. Burgess, E. Carmo-Silva, T. Lawson, A.P. De Souza, L. Leonelli, Y. Wang, Into the shadows and back into sunlight: photosynthesis in fluctuating light, *Annu. Rev. Plant Biol.* 73 (2022) 617–648.
- [38] T. Mesa, S. Munné-Bosch,  $\alpha$ -Tocopherol in chloroplasts: nothing more than an antioxidant? *Curr. Opin. Plant Biol.* 74 (2023) 102400.
- [39] A. Cortleven, S. Nitschke, M. Klauumünzer, H. Abdelgawad, H. Asard, B. Grimm, M. Riefler, T. Schmülling, A novel protective function for cytokinin in the light

- stress response is mediated by the ARABIDOPSIS HISTIDINE KINASE2 and ARABIDOPSIS HISTIDINE KINASE3 receptors, *Plant Physiol.* 164 (2014) 1470.
- [40] A. Cortleven, J.E. Leuendorf, M. Frank, D. Pezzetta, S. Bolt, T. Schmülling, Cytokinin action in response to abiotic and biotic stresses in plants, *Plant Cell Environ.* 42 (2019) 998–1018.
- [41] H.N. Nguyen, N. Lai, A.B. Kisiala, R.J.N. Emery, Isopentenyltransferases as master regulators of crop performance: their function, manipulation, and genetic potential for stress adaptation and yield improvement, *Plant Biotechnol. J.* 19 (2021) 1297–1313.
- [42] P.P. Pashkovskiy, R. Vankova, I.E. Zlobin, P. Dobrev, A.V. Kartashov, A.I. Ivanova, V.P. Ivanov, S.I. Marchenko, D.I. Nartov, Y.V. Ivanov, et al., Hormonal responses to short-term and long-term water deficit in native Scots pine and Norway spruce trees, *Environ. Exp. Bot.* 195 (2022) 104789.
- [43] G. Jammnická, H. Húdoková, P. Fleischer, M. Ježík, Soil drought stress and high-temperature effects on photosystem II in different juvenile spruce provenances, *Cent.Eur.For.J.* 70 (2024) 95–106.
- [44] M. Grieco, V. Roustan, G. Dermendjiev, S. Rantala, A. Jain, M. Leonardelli, K. Neumann, V. Berger, D. Engelmeier, G. Bachmann, et al., Adjustment of photosynthetic activity to drought and fluctuating light in wheat, *Plant Cell Environ.* 43 (2020) 1484–1500.
- [45] H. Sapeta, M. Yokono, A. Takabayashi, Y. Ueno, A.M. Cordeiro, T. Hara, A. Tanaka, S. Akimoto, M.M. Oliveira, R. Tanaka, Reversible down-regulation of photosystems I and II leads to fast photosynthesis recovery after long-term drought in *Jatropha curcas*, *J. Exp. Bot.* 74 (2023) 336–351.
- [46] L. Taiz, E. Zeiger, I.M. Møller, A. Murphy, *Plant Physiology*, Sinauer Associates Inc., U.S., 2010.
- [47] M. Li, C. Kim, Chloroplast ROS and stress signaling, *Plant. Communications.* 3 (2022) 100264.
- [48] K. Maxwell, G.N. Johnson, Chlorophyll fluorescence—a practical guide, *J. Exp. Bot.* 51 (2000) 659–668.
- [49] I. Sperdouli, J. Moustaka, O. Antonoglou, I.S. Adamakis, C. Dendrinou-samara, M. Moustakas, Leaf age-dependent Effects of foliar-sprayed CuZn generation in *Arabidopsis thaliana*, *Materials* (2019) 1–17.
- [50] P.J. Gollan, S. Grebe, L. Roling, B. Grimm, C. Spetea, E.M. Aro, Photosynthetic and transcriptome responses to fluctuating light in *Arabidopsis thaliana* ion transport triple mutant, *Plant Direct* 7 (2023) 1–16.
- [51] A. Gupta, A. Rico-Medina, A.I. Caño-Delgado, The physiology of plant responses to drought, *Science* 368 (2020) 266–269.
- [52] G. Agati, C. Brunetti, A. Fini, A. Gori, L. Guidi, M. Landi, F. Sebastiani, M. Tattini, Are flavonoids effective antioxidants in plants? Twenty years of our investigation, *Antioxidants* 9 (2020) 1–17.
- [53] M.L.F. Ferreyra, P. Serra, P. Casati, Recent advances on the roles of flavonoids as plant protective molecules after UV and high light exposure, *Physiol. Plantarum* 173 (2021) 736–749.
- [54] L. Baozhu, F. Ruonan, F. Yanting, L. Runan, Z. Hui, C. Tingting, L. Jiong, L. Han, Z. Xiang, S. Chun-peng, The flavonoid biosynthesis regulator PFG3 confers drought stress tolerance in plants by promoting flavonoid accumulation, *Environ. Exp. Bot.* 196 (2022) 104792.
- [55] J. Huang, A. Hammerbacher, A. Weinhold, M. Reichelt, G. Gleixner, T. Behrendt, N.M. van Dam, A. Sala, J. Gershenzon, S. Trumbore, et al., Eyes on the future – evidence for trade-offs between growth, storage and defense in Norway spruce, *New Phytol.* 222 (2019) 144–158.
- [56] A. Hammerbacher, L.P. Wright, J. Gershenzon, *Spruce Phenolics: Biosynthesis and Ecological Functions*, 2020, pp. 193–214.
- [57] S. Netherer, D. Kandasamy, A. Jirosová, B. Kalinová, M. Schebeck, F. Schlyter, Interactions among Norway spruce, the bark beetle *Ips typographus* and its fungal symbionts in times of drought, *J. Pest. Sci.* 94 (2021) 591–614.
- [58] A. Ganthaler, A. Guggenberger, W. Stöggli, I. Kranner, S. Mayr, Elevated nutrient supply can exert worse effects on Norway spruce than drought, viewed through chemical defence against needle rust, *Tree Physiol.* (2023) 1745–1757.